



Article

A Numerical and Experimental Investigation into the Impact Response of Sandwich Composites under Different Boundary Conditions

Dianshi Feng ¹, Gabriela Loi ² and Francesco Aymerich ^{2,*}

¹ College of Civil Engineering, Taiyuan University of Technology, Taiyuan 033024, China; fengdianshi@tyut.edu.cn

² Department of Mechanical, Chemical and Materials Engineering, University of Cagliari, 09123 Cagliari, Italy; gabriela.loi@unica.it

* Correspondence: francesco.aymerich@dimcm.unica.it

Abstract: The paper reports the results of an experimental and numerical investigation into the effect of the support conditions on the low velocity impact behaviour of sandwich composite panels. Significant differences are observed experimentally between the structural and damage responses to impact of small-span and large-span sandwich panels. In particular, impact events on large-span panels generate lower peak forces, larger displacements and smaller damage sizes in comparison to small-span panels subjected to the same impact energy. The experimental results are employed to validate the capability of a finite element (FE) tool to simulate the impact behaviour of the sandwich panels for the different boundary conditions. The comparison of FE and experimental results shows that the model provides a good prediction of the structural response as well as of the extent and mechanisms of impact damage for both small-span and large-span lengths, thus demonstrating the potential of the FE tool for verification and design of sandwich components in real engineering applications.

Keywords: sandwich composites; low velocity impact; boundary conditions; FE simulation



Citation: Feng, D.; Loi, G.; Aymerich, F. A Numerical and Experimental Investigation into the Impact Response of Sandwich Composites under Different Boundary Conditions. *J. Compos. Sci.* **2022**, *6*, 88. <https://doi.org/10.3390/jcs6030088>

Academic Editors: Francesco Tornabene and Thanasis Triantafyllou

Received: 18 February 2022

Accepted: 9 March 2022

Published: 11 March 2022

Publisher's Note: MDPI stays neutral with regard to jurisdictional claims in published maps and institutional affiliations.



Copyright: © 2022 by the authors. Licensee MDPI, Basel, Switzerland. This article is an open access article distributed under the terms and conditions of the Creative Commons Attribution (CC BY) license (<https://creativecommons.org/licenses/by/4.0/>).

1. Introduction

Over the years, composite sandwich structures, where two composite skins (or facings) are bonded to a lightweight core, have been increasingly used in various areas, ranging from civil and automotive sectors to aerospace and marine applications, because of their high strength-to-weight and stiffness-to-weight ratios, excellent energy-absorbing capability and good corrosion properties [1]. A major limitation of sandwich composites is their high vulnerability to localised damage caused by foreign object impacts, which inevitably occur during manufacturing, transport, construction and maintenance [2]. In particular, the damage generated by low-velocity impacts may be difficult or impossible to detect by visual inspection, since it often initiates and grows within the impacted composite facing without any evident dent or crack on the surface. This type of damage, known in aerospace applications as barely visible impact damage—BVID [3], can have a detrimental effect on the strength of the sandwich composite and lead to the ultimate collapse of the whole structure [4].

In recent years, the need to prevent failures and reduce the extent of costly and time-consuming experimental testing has called for reliable simulation and design tools capable of predicting the damage generated by impacts on sandwich composite structures. For this reason, a number of combined experimental and numerical investigations have been conducted to characterize the response of sandwich composites to low-velocity impacts as a preliminary step for the development and validation of physically-based damage modelling approaches. A significant amount of this research work has specifically addressed the

impact damage behaviour of sandwich composites with polymeric foam cores, which have gained considerable interest due to their low weight, limited cost, easy assembly process and excellent acoustic and thermal insulation properties [5–7].

The damage introduced by low-velocity impacts in foam-cored sandwich composites usually exhibits a complex pattern, consisting of a combination of failure modes, such as delaminations, matrix cracks, fibre fracture, foam crushing and face-core debonding. Both the extent and the typical features of this damage are strongly dependent not only on the properties of the composite facings and of the foam core, but also on the size and boundary conditions of the impacted sandwich panel.

Various studies have been, for example, conducted to examine the influence of the foam density on the structural response and on the damage mechanisms of sandwich composites subjected to impact. It is generally acknowledged that the resistance to impact damage is improved by increasing the stiffness and the strength of the core, with specimens with lower density foam core exhibiting lower threshold energy for damage initiation and more extensive damage areas than specimens with higher density cores [8–11]. The gain in damage resistance of composite sandwiches observed with increasing foam density can be attributed to the improved support provided by denser and stiffer foam cores to the impacted skin. On the other hand, the thickness of the core was seen to have a significant influence on the damage extent only for thicknesses below a certain limit value [4,12], as a consequence of the increasing importance of the overall bending deformation with decreasing core thicknesses.

The impact behaviour of sandwich composites was also observed to be greatly affected by the characteristics of the composite facings [7,13–16]; layup, thickness and ply properties playing a key role in controlling the structural response (peak load, impact duration, force history, etc.) and the damage resistance (in terms of nature, extent and through thickness distribution of the different failure modes) of the sandwich material.

Even though a variety of analytical and numerical approaches have been proposed to model impact damage in sandwich composites [2,17,18], the complexity of the failure mechanisms and the strong nonlinearity of the material response generally requires the use of finite element (FE) tools to achieve an accurate prediction of the initiation, evolution and interaction of the different damage modes occurring during the impact event. FE models that combine stress/strain failure criteria (to identify damaged elements) with element deletion or sudden stiffness reduction schemes (to introduce the degradation of material properties due to damage) have been adopted in various studies to examine the response to impact of sandwich panels or beams [14,19,20]. Within this modelling strategy, shell elements have often been chosen to reproduce the behaviour of the composite skins to reduce the computational cost. As an example, Shokrieh and Fakhar [20] used 4-node shell elements for the skins and 8-node solid elements for the core to analyse the impact behaviour of sandwich composites with glass/epoxy skins bonded to a PVC foam core. The Chang–Chang model was applied to predict the occurrence of intralaminar damage (fibre fracture and matrix cracks) within the skins, while the foam core was modelled as an elastic–plastic material. A similar modelling scheme, where the Hashin failure criterion was used to detect damage initiation, was followed in [21] to simulate the impact response of sandwich plates with carbon/epoxy skins and polyurethane foam.

In recent years, more advanced progressive damage models, in which the application of failure criteria to predict damage initiation is associated with procedures for continuous degradation of material properties [22,23], have been increasingly employed to investigate the low-velocity impact behaviour of sandwich composites. A general strategy that has become frequently adopted to simulate damage in the composite skins involves the combined use of continuum damage mechanics (CDM) methods [24] to model in-ply matrix cracking and fibre fracture with cohesive elements [25] to represent cracks at locations known a priori, such as delaminations at interfaces between layers of different orientations. Energy-based procedures are generally incorporated in both CDM and cohesive models to introduce a gradual decrease of the elastic properties due to damage [22]. Crush-

able foam models are typically applied to represent the inelastic behaviour of the foam core. Several investigations based on this modelling framework have been reported in the literature for the simulation of low-velocity impact damage in foam cored sandwich composite plates [11,13,15,26–31]. The predictions of these studies generally show a good agreement with experimental data in terms of structural behaviour as well as damage features and extent. However, a critical aspect of these analyses is that the development and validation of the models have been carried out by comparing the simulated and experimental responses of small-scale samples supported on short-span lengths. As a matter of fact, the comparisons presented in the references cited above [11–16,20,21,26–31] were all based on experiments on sandwich plates positioned over rectangular or circular openings with sizes ranging between 45 and 125 mm or even fully supported on a rigid base. Experimental evidence shows however that the span length plays a key role in the impact response of sandwich beams and plates [32,33], which appears to be essentially controlled by local indentation effects for small-span lengths but greatly affected by the dynamic deformation behaviour of the overall plate for large-span conditions. For a reliable use of simulation tools in the design phase of sandwich composite components, it is therefore important to evaluate the predictive quality of the numerical models not only for impacts on small scale samples but also for sizes and loading conditions more representative of real engineering applications.

In this study, a series of impact tests were carried out at different energies on foam-based sandwich panels with two different sizes and span lengths, specifically chosen to achieve impact responses that vary from those dominated by local material properties at the contact region (i.e., for small spans) to those involving the crucial effect of the global dynamic deformation of the sandwich plate (for large spans). Experimental data and observations collected for the two different boundary conditions were used to verify the performance of an FE model previously developed by the authors to predict the structural behaviour and damage resistance of impacted sandwich composites. The results of the FE analyses were compared to the experimental outcomes on the basis of a number of relevant validation metrics (force histories, force-deflection curves, damage size and pattern) to assess the reliability of the simulations for the two different (global vs. local) response domains.

2. Materials and Experimental Testing

Sandwich panels made of composite skins bonded to a polymeric foam core were manufactured for this investigation. The facing skins of the panels consisted of ten plies of unidirectional carbon/epoxy prepreg (Texipreg HS300/ET223 by Seal, Legnano, Italy) laid up in a $[0_3/\pm 45]_s$ stacking sequence. Individual plies had a fibre volume ratio of 0.62 and a nominal thickness of 0.32 mm. The core material was a closed-cell PVC foam (Divinycell HP) with a thickness of 20 mm. Divinycell HP is a foam specifically developed for compatibility with low-medium temperature prepreg systems, which may be processed at temperatures up to 145 °C and is capable of continuous operation in a temperature range between –200 and 80 °C [34]. Foams with densities of 65 kg/m³ (HP60) and 160 kg/m³ (HP160) were used for the sandwich core.

The panels were consolidated in a vacuum-bag through a co-curing process, during which bonding of the composite skins to the foam core was achieved simultaneously with the curing of the prepreg layers without the use of additional adhesive material. The thermal cycle consisted of a 25 min heating stage up to 100 °C, followed by a dwell time of 6 h and a final cooling stage to room temperature maintaining vacuum. Panels with 250 mm × 250 mm and 350 mm × 350 mm planar sizes were manufactured to examine the impact response of the sandwich composites and to validate the predictive quality of the FE model for impacts on both small-span and large-span boundary conditions.

The impact tests were conducted using an instrumented drop-weight testing machine equipped with a 2.34 kg impactor provided with a 12.5 mm hemispherical indenter. A pneumatic braking system integrated within the testing rig was used to stop the

impactor after the rebound so as to prevent multiple impacts on the specimen. During impact, the 250 mm × 250 mm panels were simply supported on a steel plate with a small 45 mm × 67.5 mm rectangular opening (small-span configuration), while the large 350 mm × 350 mm panels were supported along two opposite sides parallel to the 0° direction, with an inner span between the supported edges of 300 mm (large-span configuration). Figure 1 shows schematics of the small-span (Figure 1a) and large-span (Figure 1b) support configurations. The sandwich panels were impacted at the centre with energy levels between 2 and 6.2 J, obtained by varying the drop height of the impactor mass. The range of impact energies was selected to approximately cover damage responses spanning from damage initiation to BVID. The contact force between the impactor and the sandwich sample was measured by a semiconductor strain-gauge bridge bonded to the indenter, while the signal from an infrared sensor was used to determine the impact and rebound velocities. The displacement of the indenter was obtained as a function of time by integration of the contact force versus time history.

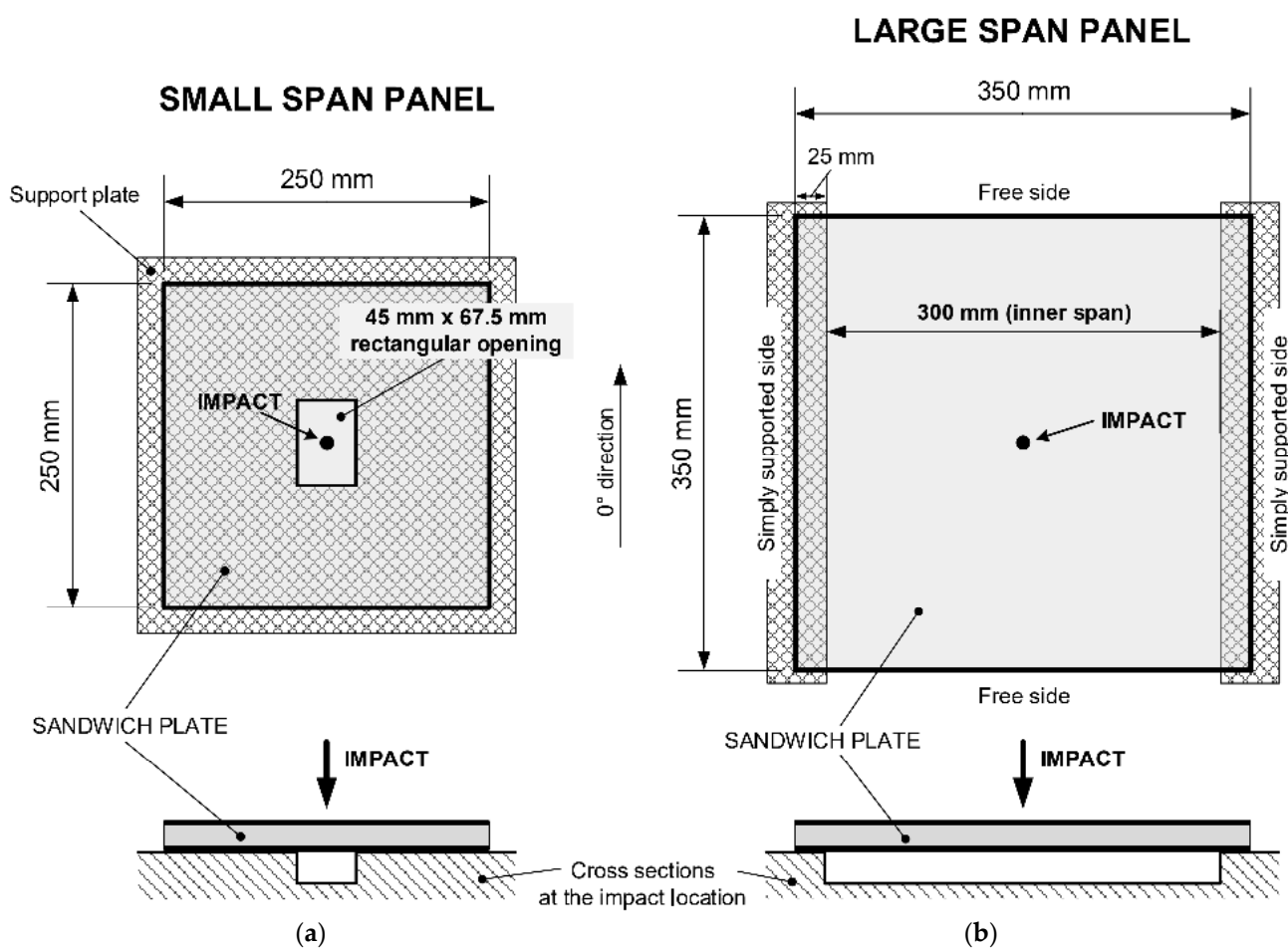


Figure 1. Geometry and support conditions of small-span (a) and large-span (b) sandwich panels.

The damage produced by the impact was assessed by visual inspection and by X-radiography enhanced by infiltration of a zinc iodide liquid solution opaque to X-rays in the damaged region. Stereoscopic X-ray observations were also made to assess the through-thickness distribution of internal damage. Ultrasonic C-scans were carried out in sandwich panels impacted at the lower energy (≈ 2 J) to obtain information on possible internal damage not connected to the external surface, which may remain undetected by X-radiography because of the impossibility of the radio-opaque liquid to fill the fracture surfaces.

3. Experimental Results

Figures 2 and 3 show force histories and force–displacement curves for impacts on sandwich panels with low density (HP60; Figure 2) and high density (HP160; Figure 3) cores. The graphs compare the impact curves of panels positioned on the 45 mm × 67.5 mm window cut-out (small-span configuration) with those of panels supported on the 300 mm span (large-span configuration).

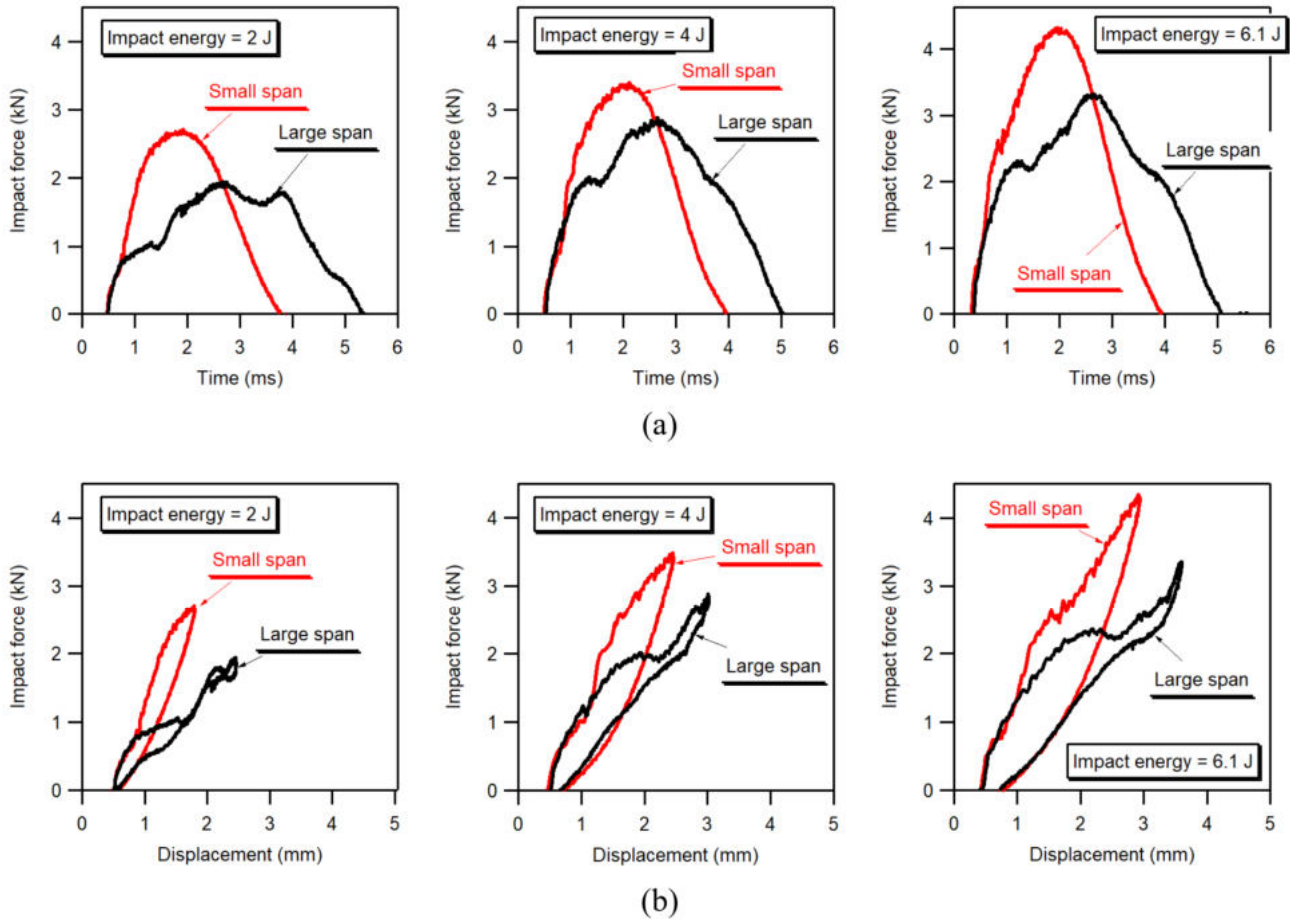


Figure 2. Force–time (a) and force–displacement (b) curves measured during impact on HP60 sandwich panels supported on large-span and small-span lengths.

It is immediately seen that, for both HP60 and HP160 sandwich composites, the structural response of panels with a large span is very different to that of panels supported on a small-span window. An evident difference concerns the general shape of the impact curves, which show fluctuating force histories for large-span panels as compared to smoother and more regular force histories for small-span panels. Furthermore, as expected, because of the lower flexural rigidity of large-span panels, impacts on panels supported on the long 300 mm span are characterized by lower peak loads, larger displacements and longer impact durations than small-span counterpart panels. The significant difference in the peak impact forces between large-span and small-span responses can be readily seen in the graphs of Figure 4, which plot the peak force values as a function of impact energy for HP60 and HP160 panels. It may be worth remarking that, because of the increased support provided by the high density HP160 foam to the impacted skin, HP160 panels exhibit a much stiffer response than corresponding HP60 panels, with higher peak loads, smaller displacements and shorter impact durations, as is easily observed by comparing the graphs of Figures 2–4.

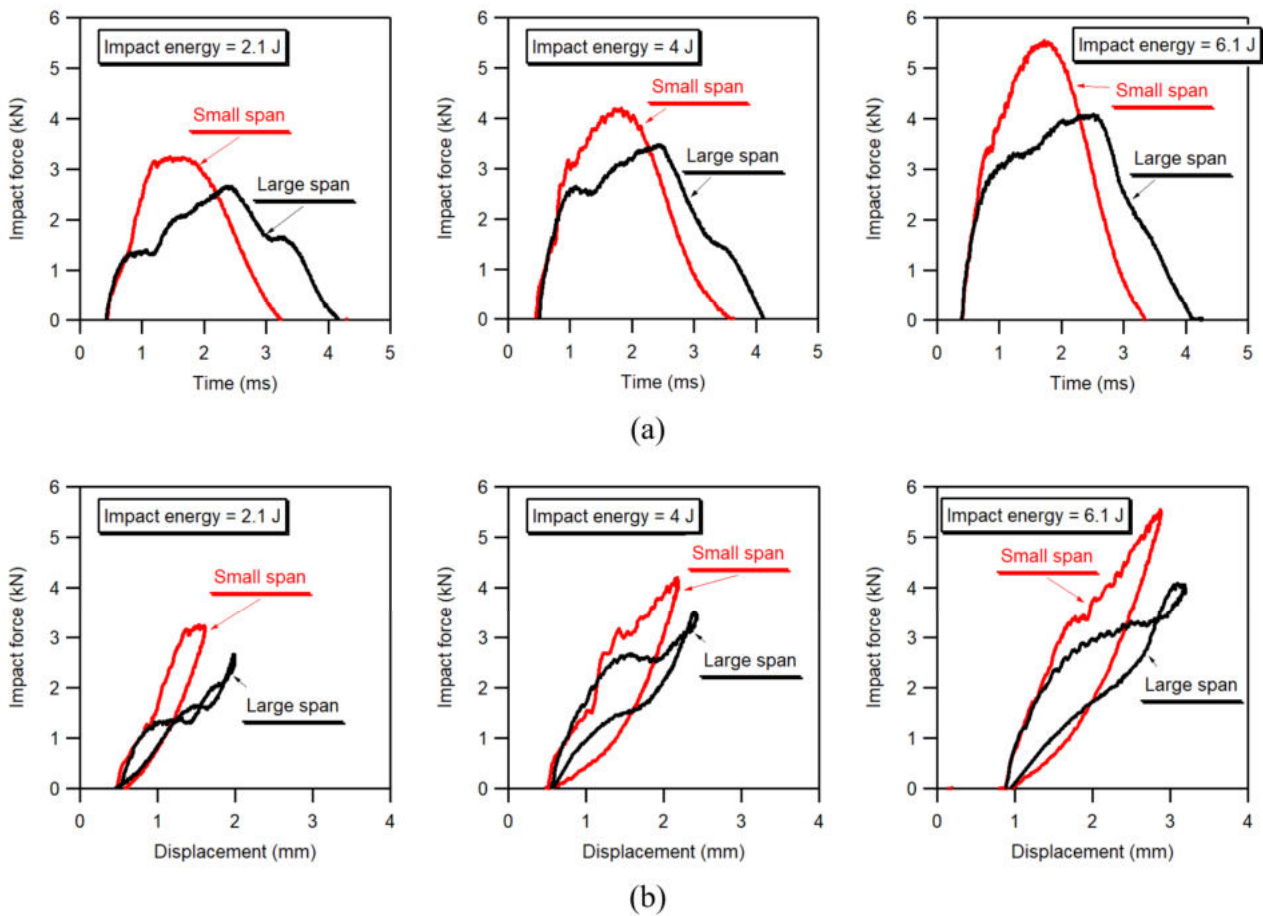


Figure 3. Force–time (a) and force–displacement (b) curves measured during impact on HP160 sandwich panels supported on large-span and small-span lengths.

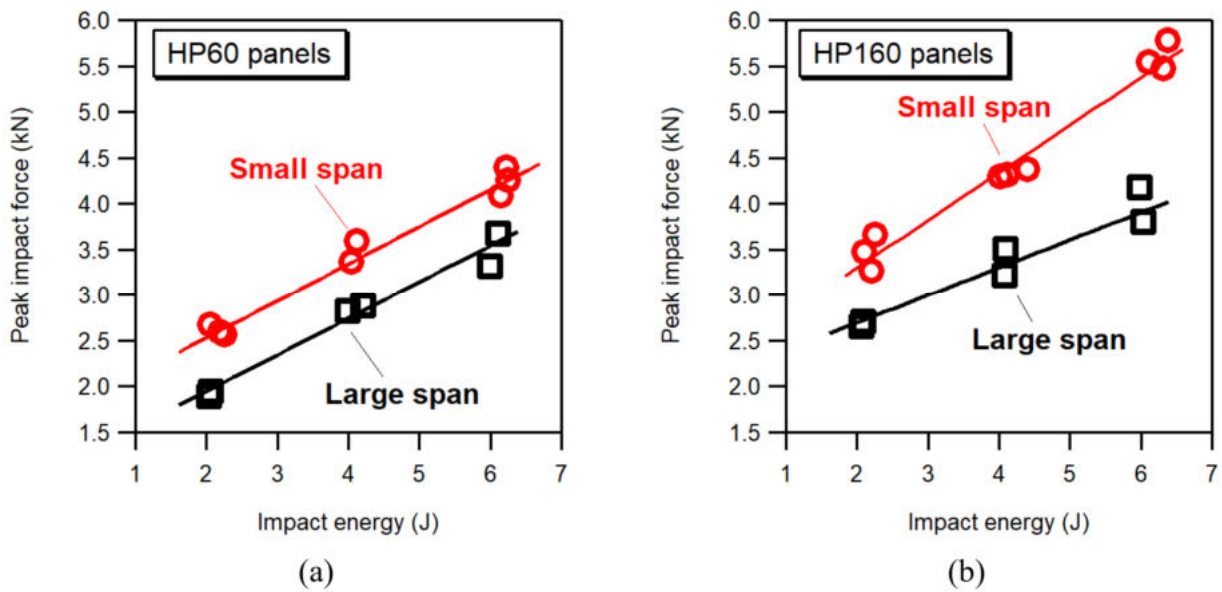


Figure 4. Peak forces vs. impact energy measured during impact on HP60 (a) and HP160 (b) sandwich panels supported on large-span and small-span lengths.

A detailed examination of the traces of Figures 2 and 3 shows that the force–time and force–displacement curves measured during impact on small-span and large-span panels have the same trend during the initial stage of contact. However, the impact responses

start to diverge considerably for larger displacements, when the large-span panels start exhibiting high-amplitude, low-frequency, force oscillations, with global force–displacement slopes significantly lower than those of small-span panels. These results clearly indicate that after the very early contact phase, during which the local indentation response dominates the interaction between the impactor and the panel, the impact behaviour becomes increasingly dependent on the boundary conditions. Therefore, the characteristic shapes of the large-span impact curves are the result of the complex combination of the local elastic and damage response to indentation, the global flexural response of the panel, and the dynamic interaction between the impactor, the target panel and the surfaces of the supporting fixture.

X-radiographs of damage induced by impacts of increasing energies on small-span and large-span lengths are shown in Figures 5 and 6, respectively, for HP60 and HP160 foam cores. The sandwich panels exhibit similar impact damage patterns, consisting of a stack of peanut-shaped delaminations that develop at different interfaces of the impacted skin, together with shear and tensile matrix cracks that affect, respectively, the central $+45^\circ / -45^\circ$ plies and the bottom 0° plies. Neither significant fibre fracture nor debonding between the core and the composite skins were observed on the impacted panels for the examined range of impact energies. It is immediately seen that, for the same impact energy, the extent of damage is significantly smaller in large-span panels than in small-span panels for both HP60 and HP160 cores. These results show that the boundary conditions play a critical role not only in controlling the structural response of the sandwich component but also in driving the onset and growth of the damage induced by the impact in the composite skin.

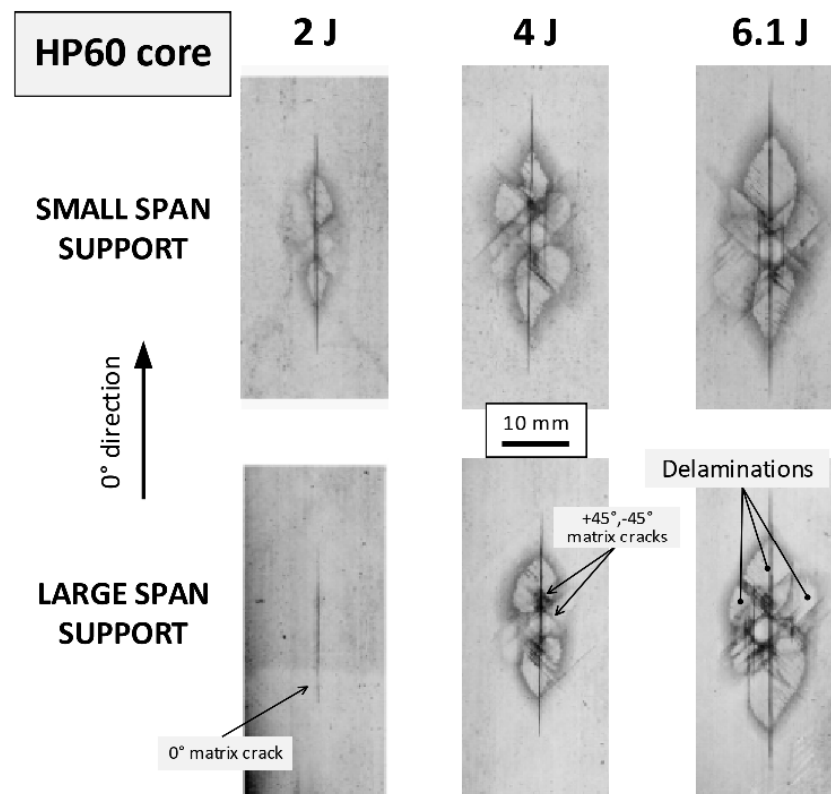


Figure 5. X-radiographs of damage in small-span (top) and large-span (bottom) HP60 sandwich panels impacted at three energy levels.

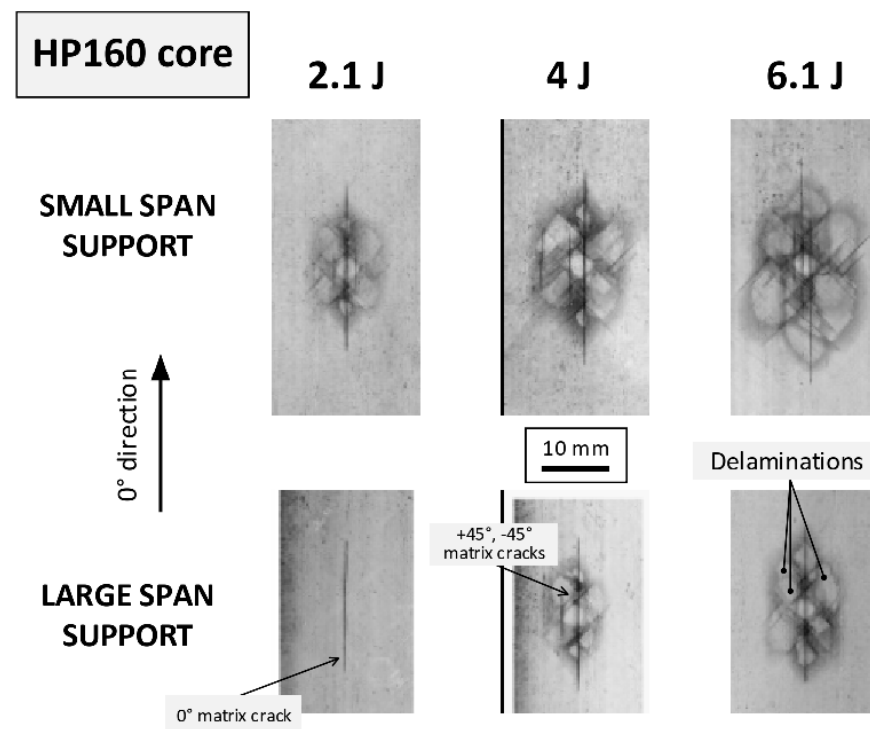


Figure 6. X-radiographs of damage in small-span (**top**) and large-span (**bottom**) HP160 sandwich panels impacted at three energy levels.

4. FE Modelling

An FE tool for the prediction of the structural and damage response of sandwich composites subjected to impact was developed and verified by the authors in previous studies by comparison with experimental results on small-span sandwich panels with different skin layups and foam core densities [11,15,30]. The numerical tool has been applied in this investigation to simulate the impact behaviour of the sandwich panels for the two support configurations (small span vs. large span) described in the previous section. The main objective of the analysis was assessing the predictive performance of the FE model when modelling impacts on structural systems in which the global deformation of the whole sandwich structure plays a major role in the response to the impact event. The data acquired during the experimental tests have been used as a reference basis to explore the robustness of the model and verify the capability of the tool to correctly capture and reproduce the change in the impact response of the sandwich composites generated by the different support conditions.

The numerical tool, which is based on the ABAQUS/Explicit solver, simulates the initiation, the growth and the interaction of the typical damage modes that develop in the composite skins by means of energy-based continuum damage mechanics models for intralaminar damage (i.e., matrix cracks and fibre fracture) and interfacial cohesive elements for interlaminar damage (delaminations). The damage models were implemented into ABAQUS/Explicit through user-defined VUMAT material subroutines. C3D8R solid elements with reduced integration and COH3D8 cohesive elements were respectively used to represent the individual layers and the interfaces between layers of different orientations. The foam material was modelled using C3D8R elements implementing a crushable foam plasticity model with volumetric hardening available in ABAQUS/Explicit. Figure 7 shows the FE model built for the simulations, where an element size of $0.5 \text{ mm} \times 0.5 \text{ mm}$ on the plane of the laminated skins was used in the fine region of the mesh.

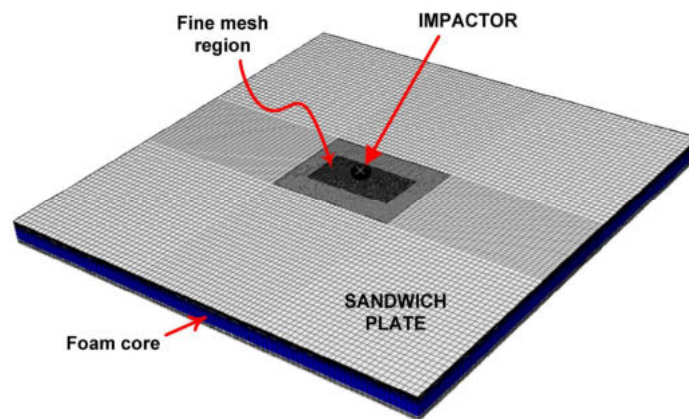


Figure 7. FE model of the 350 mm × 350 mm large-span sandwich panels.

A detailed description of the mesh geometry, material models and numerical setups adopted for the FE analyses, as well as of the experimental tests performed to measure the entire set of material properties used in the FE calculations, can be found in [15].

5. Comparison between Numerical and Experimental Results

Experimental and simulated force–time and force–displacement curves for three energy levels are plotted in the graphs of Figures 8–11. Figures 8 and 9 compare the numerical and measured responses to impact of panels with HP60 foam core. Analogous comparisons are shown in Figures 10 and 11 for panels with HP160 foam core.

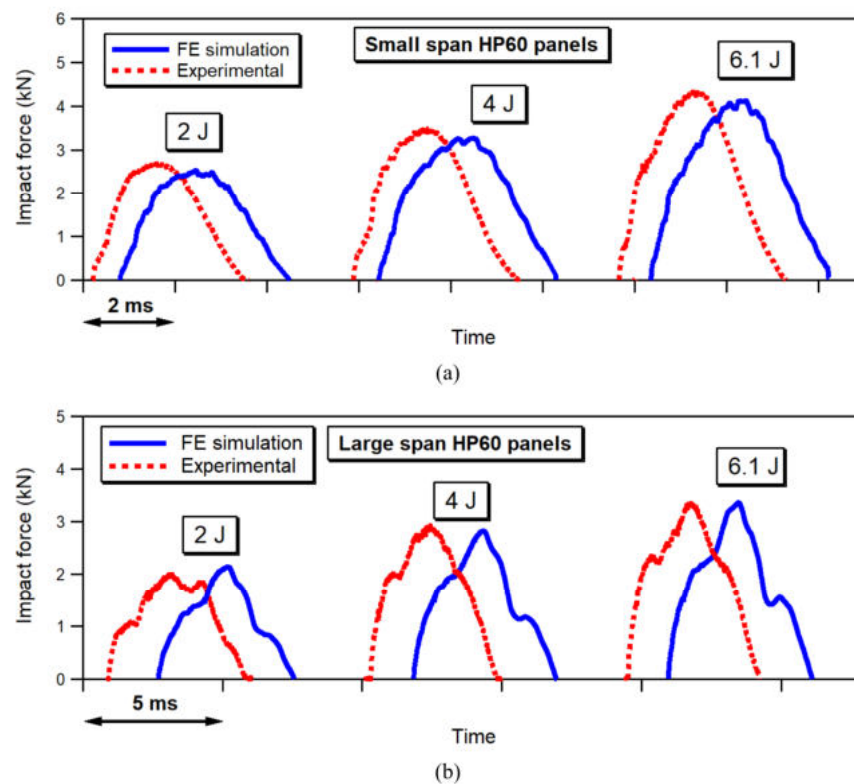


Figure 8. Comparison of simulated and experimental force–time curves for impacts on small-span (a) and large-span (b) sandwich panels with HP60 foam core.

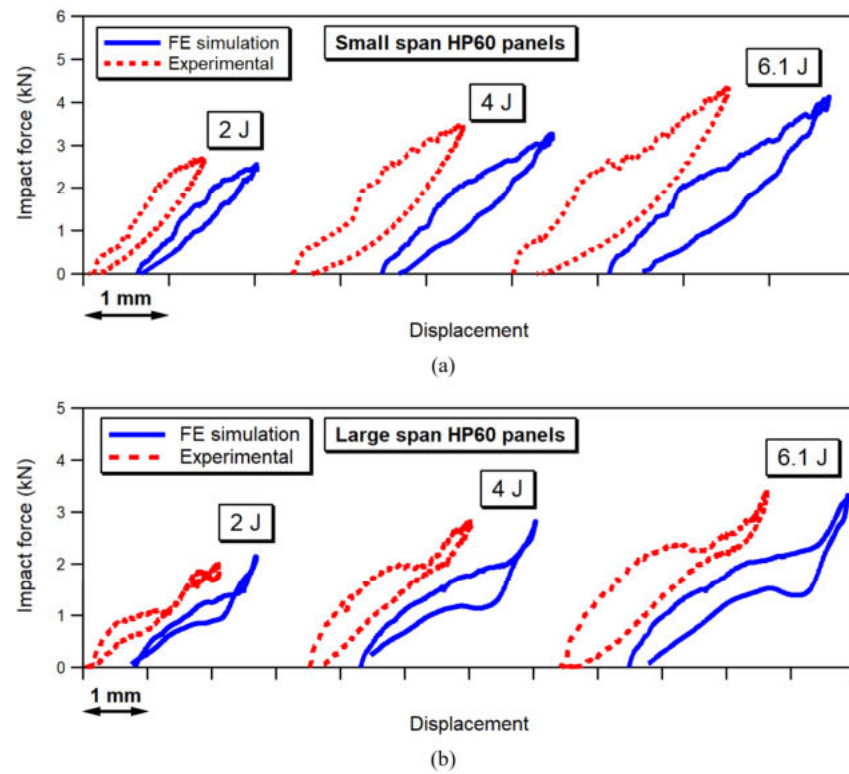


Figure 9. Comparison of simulated and experimental force–displacement curves for impacts on small-span (a) and large-span (b) sandwich panels with HP60 foam core.

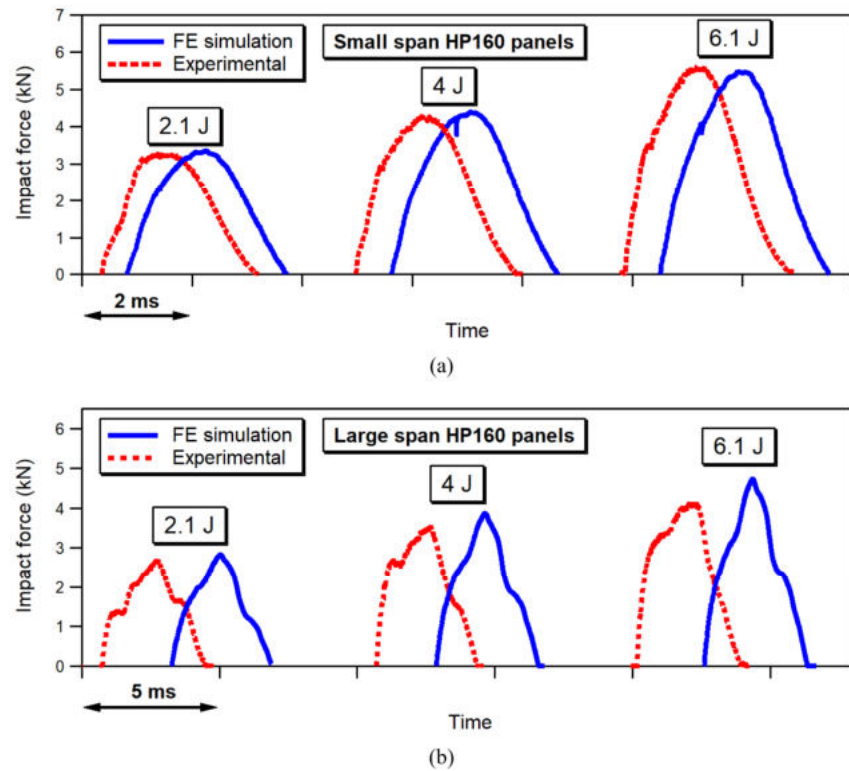


Figure 10. Comparison of simulated and experimental force–time curves for impacts on small-span (a) and large-span (b) sandwich panels with HP160 foam core.

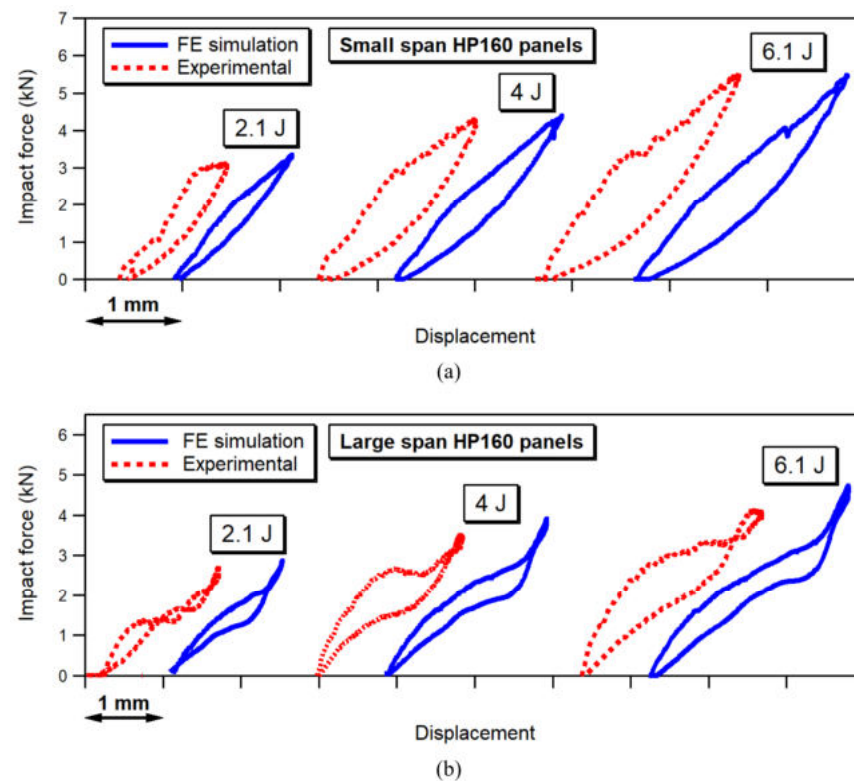


Figure 11. Comparison of simulated and experimental force–displacement curves for impacts on small-span (a) and large-span (b) sandwich panels with HP160 foam core.

It may be seen that a rather good agreement is achieved in terms of force–time histories and force–displacement curves between FE simulations and experiments for both small-span and large-span boundary conditions. We may notice that the FE model correctly captures the drastic modification of the response of the sandwich plates when the boundary conditions are changed from the small-span to the large-span support. In particular, the graphs of Figures 8a–11a show that the impact curves obtained when modelling impacts on small-span panels exhibit a rather smooth trend, which is indicative of a structural behaviour essentially controlled by the localized material response at the contact region. On the other hand, the FE simulations of impacts on large-span panels, presented in the graphs of Figures 8b–11b, show that the model is able to reproduce the peculiar shape of the force–time and force–displacement curves, by correctly replicating the presence of the high-amplitude, low-frequency, force fluctuations due to the dynamic oscillation of the whole panel induced by the impulsive load.

The predictive performance of the model is summarized in terms of peak force in the graphs of Figure 12, where the maximum forces measured during impact on small-span and large-span panels are plotted as a function of impact energy for HP60 (Figure 12a) and HP160 (Figure 12b) sandwich panels. The graphs show that a rather good correlation is achieved between simulated and experimental peak impact forces for the different boundary configurations, foam core densities and impact energies, even though the FE model tends to slightly overestimate the peak forces of large-span HP 160 panels at higher impact energies. It is seen, in particular, that the FE analyses reproduce correctly, for both HP60 and HP160 sandwich composites, the reduction in the peak forces measured on large-span panels as compared to small-span panels, thus confirming the effectiveness of the tool in properly accounting for the global dynamic response to impact of the structure.

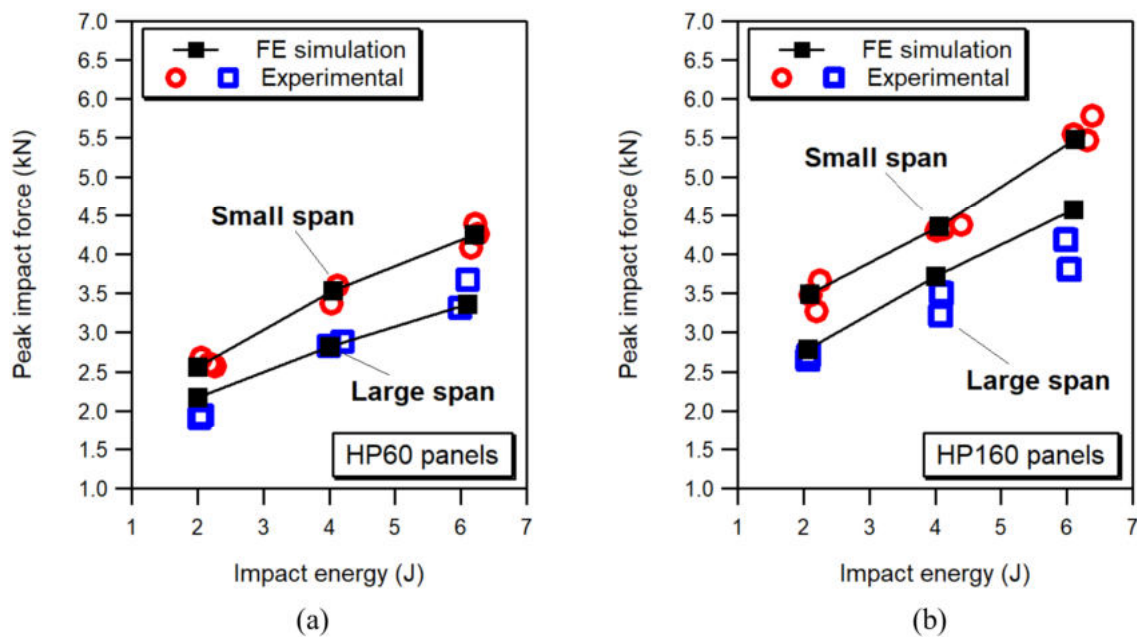


Figure 12. Comparison of simulated and experimental peak contact forces for small-span and large-span sandwich panels with HP60 (a) and HP160 (b) foam cores.

Figures 13 and 14 compare images of impact damage as revealed by X-radiography with damage maps obtained by the FE analyses, where the different grey levels correspond to different damage depths. We may see that the FE model produces a faithful description of the damage pattern of the HP60 and HP160 sandwich panels for both the small-span and large-span support conditions. The FE simulations provide an adequate prediction not only of the planar size and of the typical shape of the impact damage, but also of the sequence of the different failure mechanisms that occur under increasing impact energy. In agreement with the experimental observations, the FE analyses predicts that damage initiates with a long matrix crack on the bottom 0° plies and small delaminations at the $+45^\circ/-45^\circ$ and $-45^\circ/+45^\circ$ interfaces. With increasing impact energies, delaminations are predicted to develop and grow at the other interfaces, along with some diffuse matrix cracking in 0° and $\pm 45^\circ$ layers, as indicated in the FE damage maps of Figures 13 and 14. The FE tool is also capable of capturing, with remarkable accuracy, the distribution of internal damage at different depths of the impacted skin, as shown in the example of Figure 15, which presents a three dimensional reconstruction of the individual failure mechanisms predicted by the FE model for a 6.1 J impact on a large-span HP160 sandwich panel.

The predictive performance of the FE model in terms of overall damage extent is illustrated in the graphs of Figure 16, which compare experimental and predicted projected damage areas for small-span and large-span panels. The projected damage areas, defined as the projection onto a single plane of the delaminated areas at all interfaces of the impacted skin, was measured on the radiographic images as the area enclosed by the contour enveloping all delaminations. The data reported in the graphs of Figure 16 show a remarkably good quantitative match between values of experimental and simulated damage areas, with the proposed FE model successfully capturing the significant difference in damage size observed, for the same impact energy level, between the large and small support configurations.

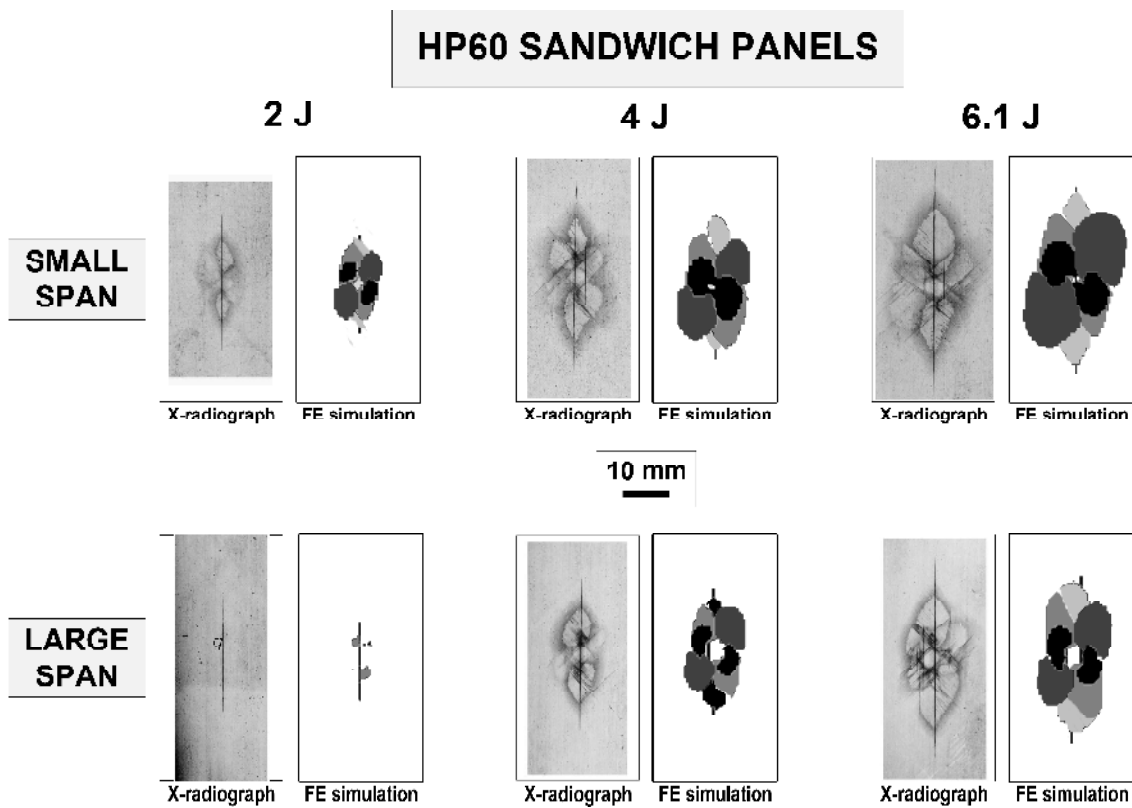


Figure 13. Comparison between experimental and predicted damage for small-span (**top**) and large-span (**bottom**) HP60 panels impacted at three energy levels. The dotted black line in the X-radiograph of the large-span panel impacted at 2 J represents the contour of the delamination as assessed by ultrasonics.

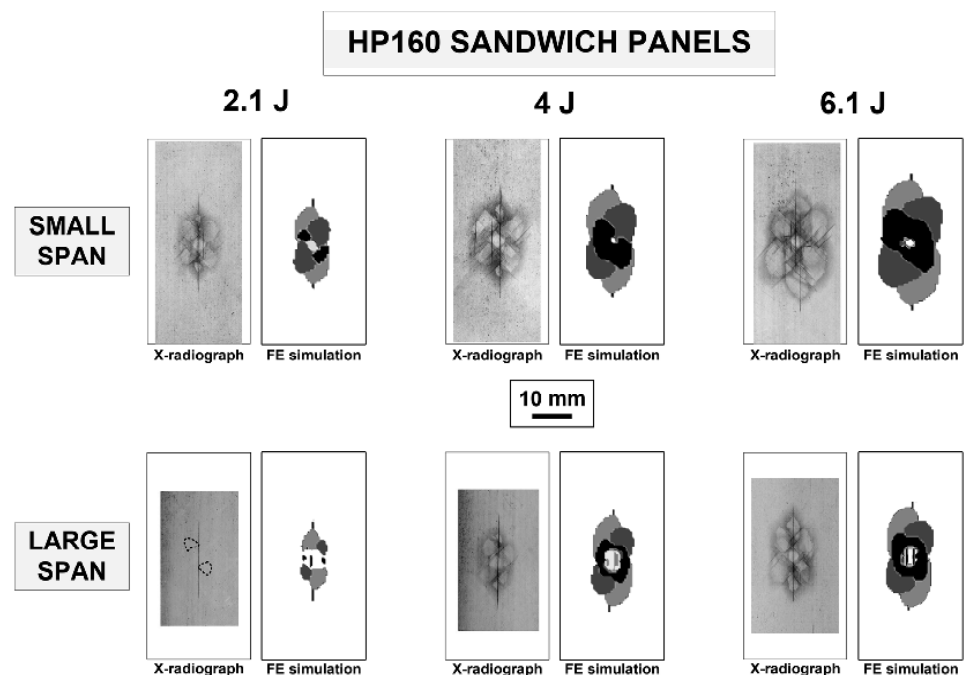


Figure 14. Comparison between experimental and predicted damage for small-span (**top**) and large-span (**bottom**) HP160 panels impacted at three energy levels. The dotted black line in the X-radiograph of the large-span panel impacted at 2.1 J represents the contour of the delaminations as assessed by ultrasonics.

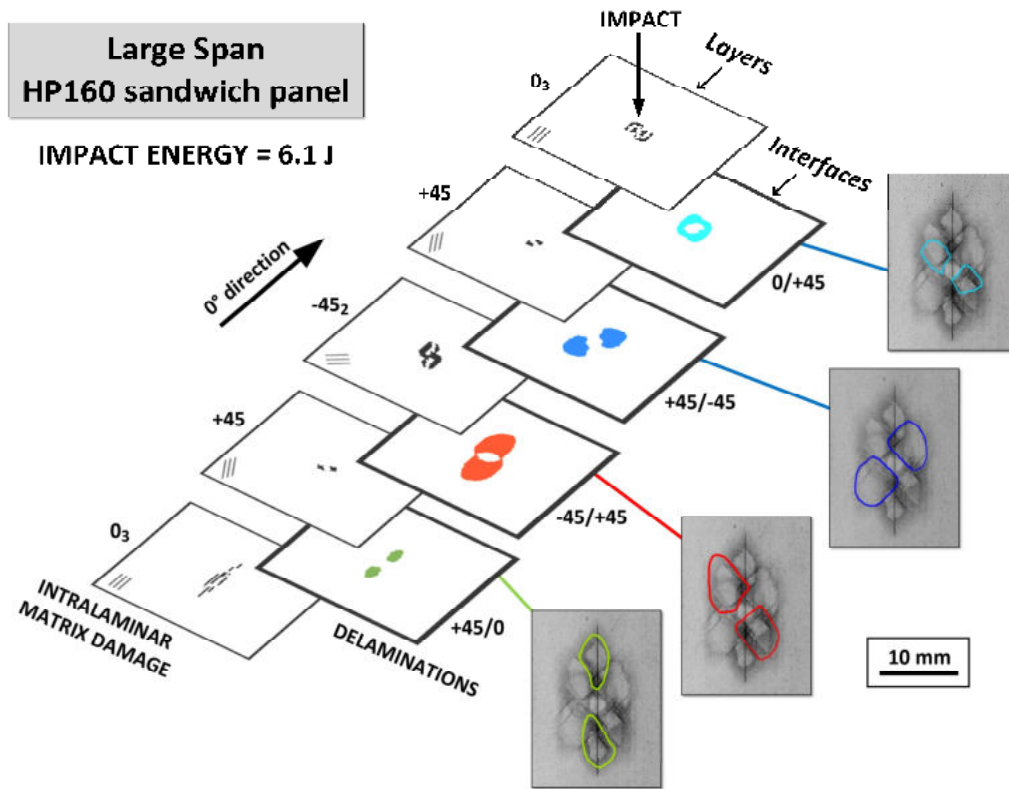


Figure 15. Comparison between experimental and predicted impact damage in a large-span sandwich panel subjected to a 6.1 J impact.

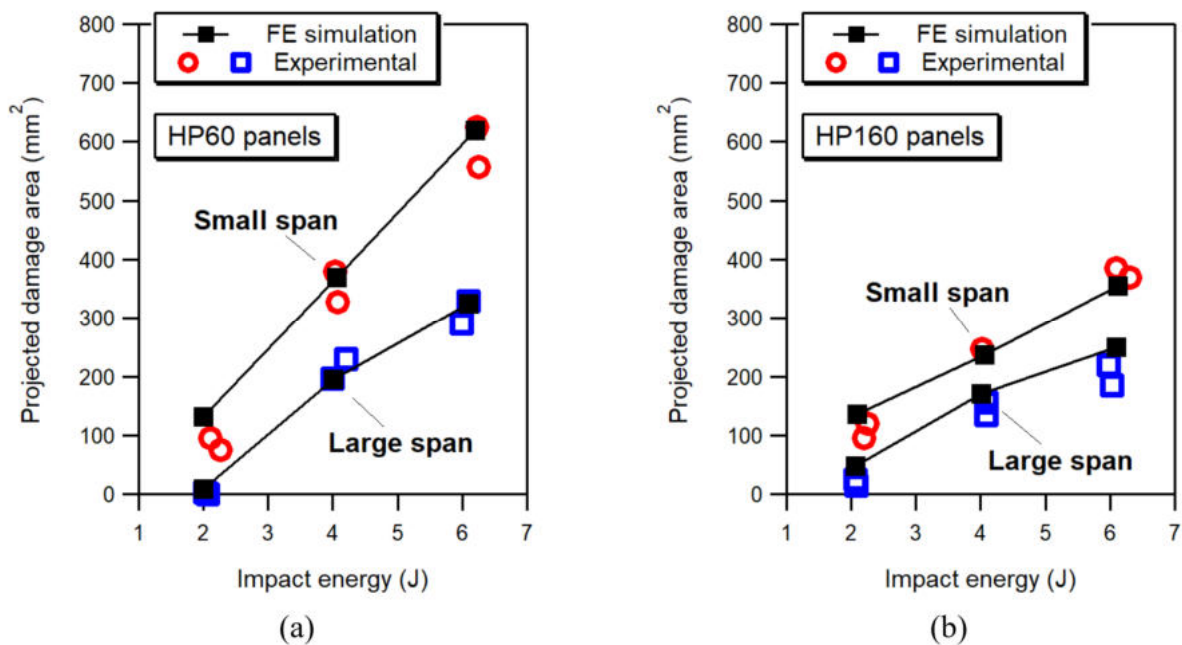


Figure 16. Comparison of simulated and experimental projected damage areas for small-span and large-span sandwich panels with HP60 (a) and HP160 (b) foam cores.

6. Conclusions

The influence of the boundary conditions on the impact behaviour of sandwich composites was examined in this study at impact energies inducing damage with different BVID severities. Panels with carbon/epoxy skins and low density (HP60) or high density

(HP160) PVC foam cores were manufactured for the impact tests. Two different support conditions (a small-span and a large-span configuration) were experimentally investigated. The relevant data collected during the experiments were used to explore the capability of an FE tool to correctly reproduce the structural behaviour of the sandwich composites over the different response scenarios associated with the two boundary conditions.

The experimental observations show that the impact response of large-span panels is significantly different from that of small-span panels. Impact events on large-span panels are characterized by lower peak forces, larger displacements and longer contact durations as compared to those of corresponding small-span panels. Furthermore, the force history measured during impact on large-span panels is strongly perturbed by high amplitude oscillations associated to the overall dynamics of the panel. In contrast, small-span panels exhibit a much smoother force history, which is essentially controlled by the local response of the material at the contact region. The support conditions also greatly affect the damage response of the sandwich composites, with extents of impact damage in large-span panels always notably smaller than those of counterpart small-span panels.

A comparison of the experimental results with the outcomes of the numerical simulations shows that the FE model predicts, with a rather good accuracy, the structural behaviour (in terms of force–time and force–displacement curves) and the damage response (damage size, individual failure mechanisms and three-dimensional pattern) of HP60 and HP160 sandwich panels for both the small-span and the large-span support conditions. The FE tool thus appears capable of simulating correctly, without any model tuning or parameter calibration, the physical mechanisms by which the support conditions affect the impact behaviour of the sandwich panels, thus suggesting the applicability of the proposed numerical approach for modelling the impact response of sandwich structures with scales and boundary conditions typical of real engineering applications. Additional experimental tests and associated FE simulations are however needed to extend the analysis to impacts with energies inducing higher damage severities, such as those involving large-scale fibre fracture or perforation/penetration conditions.

Author Contributions: Conceptualization, D.F., G.L. and F.A.; methodology, D.F., G.L. and F.A.; software, D.F.; validation, D.F., G.L. and F.A.; investigation, D.F., G.L. and F.A.; writing, D.F., G.L. and F.A.; supervision, F.A. All authors have read and agreed to the published version of the manuscript.

Funding: This research was partially supported by the EU funded FP7-ITN-Marie Curie project SYSWIND (grant No. FP7-PEOPLE-ITN 238325). D.F. would also like to thank the support by Scientific and Technological Innovation Programs of Higher Education Institutions in Shanxi (2019L0203).

Data Availability Statement: The data presented in the paper are available upon request.

Conflicts of Interest: The authors declare no conflict of interest.

References

1. Birman, V.; Kandomateas, G.A. Review of current trends in research and applications of sandwich structures. *Compos. B. Eng.* **2018**, *142*, 221–240. [[CrossRef](#)]
2. Chai, G.B.; Zhu, S. A review of low-velocity impact on sandwich structures. *Proc. Inst. Mech. Eng. Part L J. Mater. Des. Appl.* **2011**, *225*, 207–230. [[CrossRef](#)]
3. James, R.; Joseph, R.P.; Giurgiutiu, V. Impact damage ascertainment in composite plates using in-situ acoustic emission signal signature identification. *J. Compos. Sci.* **2021**, *5*, 79. [[CrossRef](#)]
4. Leijten, J.; Bersee, H.E.N.; Bergsma, O.K.; Beukers, A. Experimental study of the low-velocity impact behaviour of primary sandwich structures in aircraft. *Compos. A Appl. Sci. Manuf.* **2009**, *40*, 164–175. [[CrossRef](#)]
5. Flores-Johnson, E.A.; Li, Q.M. Low velocity impact on polymeric foams. *J. Cell. Plast.* **2011**, *1*, 45–63. [[CrossRef](#)]
6. Xiong, J.; Du, Y.; Mousanezhad, D.; Eydani, A.M.; Norato, J.; Vaziri, A. Sandwich structures with prismatic and foam cores: A review. *Adv. Eng. Mater.* **2019**, *1*, 1800036. [[CrossRef](#)]
7. Kahn, M.H.; Li, B.; Tan, K.T. Impact performance and bending behavior of carbon-fiber foam-core sandwich composite structures in cold arctic temperature. *J. Compos. Sci.* **2020**, *4*, 133. [[CrossRef](#)]
8. Anderson, T.; Madenci, E. Experimental investigation of low-velocity impact characteristics of sandwich composites. *Compos. Struct.* **2000**, *50*, 239–247. [[CrossRef](#)]

9. Hazizan, M.A.; Cantwell, W.J. The low velocity impact response of foam-based sandwich structures. *Compos. B. Eng.* **2002**, *33*, 193–204. [[CrossRef](#)]
10. Daniel, I.M. Impact response and damage tolerance of composite sandwich structures. In *Dynamic Failure of Materials and Structures*; Shukla, A., Ravichandran, G., Rajapakse, Y., Eds.; Springer: New York, NY, USA, 2010.
11. Feng, D.; Aymerich, F. Effect of core density on the low-velocity impact response of foam-based sandwich composites. *Compos. Struct.* **2020**, *239*, 112040. [[CrossRef](#)]
12. Ozdemir, O.; Karakuzu, R.; Al-Shamary, A.K.J. Core-thickness effect on the impact response of sandwich composites with poly (vinyl chloride) and poly (ethylene terephthalate) foam cores. *J. Compos. Mater.* **2015**, *49*, 1315–1329. [[CrossRef](#)]
13. Wang, J.; Waas, A.M.; Wang, H. Experimental and numerical study on the low-velocity impact behavior of foam-core sandwich panels. *Compos. Struct.* **2013**, *96*, 298–311. [[CrossRef](#)]
14. Mohammed, R.; Zhang, F.; Sun, B.; Gu, B. Finite element analyses of low-velocity impact damage of foam sandwiched composites with different ply angles face sheets. *Mater. Des.* **2013**, *47*, 189–199. [[CrossRef](#)]
15. Feng, D.; Aymerich, F. Damage prediction in composite sandwich panels subjected to low velocity impact. *Compos. A Appl. Sci. Manuf.* **2013**, *52*, 12–22. [[CrossRef](#)]
16. Atas, C.; Potoglu, U. The effect of face-sheet thickness on low-velocity impact response of sandwich composites with foam cores. *J. Sandw. Struct.* **2016**, *18*, 215–228. [[CrossRef](#)]
17. Abrate, S. Localized impact on sandwich structures with laminated facings. *Appl. Mech. Rev.* **1997**, *50*, 69–97. [[CrossRef](#)]
18. Castaniè, B.; Bouvet, C.; Ginot, M. Review of composite sandwich structure in aeronautic applications. *Compos. Part C Open Access* **2020**, *1*, 100004. [[CrossRef](#)]
19. Icardi, U.; Ferrero, L. Impact analysis of sandwich composites based on a refined plate element with strain energy updating. *Compos. Struct.* **2009**, *89*, 35–51. [[CrossRef](#)]
20. Shokrieh, M.M.; Fakhar, M.N. Experimental, analytical, and numerical studies of composite sandwich panels under low-velocity impact loadings. *Mech. Compos. Mater.* **2012**, *47*, 643–658. [[CrossRef](#)]
21. Long, S.; Yao, X.; Wang, H.; Zhang, X. Failure analysis and modeling of foam sandwich laminates under impact loading. *Compos. Struct.* **2018**, *197*, 10–20. [[CrossRef](#)]
22. Garnich, M.R.; Akula, V.M.K. Review of degradation models for progressive failure analysis of fiber reinforced polymer composites. *Appl. Mech. Rev.* **2009**, *62*, 010801. [[CrossRef](#)]
23. Rose, C.A.; Dávila, C.G.; Leone, F.A. Analysis Methods for Progressive Damage of Composite Structures. NASA/TM–2013-218024. 2013. Available online: <https://ntrs.nasa.gov/api/citations/20140001002/downloads/20140001002.pdf> (accessed on 17 February 2022).
24. Forghani, A.; Shahbazi, M.; Zobeiry, N.; Poursartip, A.; Vaziri, R. An overview of continuum damage models used to simulate intralaminar failure mechanisms in advanced composite materials. In *Numerical Modelling of Failure in Advanced Composite Materials*; Woodhead Publishing Series in Composites Science and Engineering; Elsevier: Duxford, UK, 2015; pp. 151–173. [[CrossRef](#)]
25. Tabiei, A.; Zhang, W. Composite laminate delamination simulation and experiment: A review of recent development. *Appl. Mech. Rev.* **2018**, *70*, 030801. [[CrossRef](#)]
26. Brooks, R.; Brown, K.A.; Warrior, N.A.; Kulandaivel, P.P. Predictive modeling of the impact response of thermoplastic composite sandwich structures. *J. Sandw. Struct. Mater.* **2010**, *12*, 449–476. [[CrossRef](#)]
27. Zhou, J.; Hassan, M.Z.; Guan, Z.; Cantwell, W.J. The low velocity impact response of foam-based sandwich panels. *Compos. Sci. Technol.* **2012**, *72*, 1781–1790. [[CrossRef](#)]
28. Yang, P.; Shams, S.S.; Slay, A.; Brokate, B.; Elhajjar, R. Evaluation of temperature effects on low velocity impact damage in composite sandwich panels with polymeric foam cores. *Compos. Struct.* **2015**, *129*, 213–223. [[CrossRef](#)]
29. He, Y.; Zhang, X.; Long, S.; Yao, X.; He, L. Dynamic mechanical behavior of foam-core composite sandwich structures subjected to low-velocity impact. *Arch. Appl. Mech.* **2016**, *86*, 1605–1619. [[CrossRef](#)]
30. Feng, D.; Aymerich, F. Experimental and numerical investigation into the damage response of composite sandwich panels to low-velocity impact. *Struct. Monit. Maint.* **2017**, *4*, 133–151. [[CrossRef](#)]
31. Rajput, M.S.; Burman, M.; Forsberg, F.; Hallstrom, S. Experimental and numerical study of the response to various impact energy levels for composite sandwich plates with different face thicknesses. *J. Sandw. Struct. Mater.* **2019**, *21*, 1654–1682. [[CrossRef](#)]
32. Shen, Y.O.; Yang, F.J.; Cantwell, W.J.; Balawi, S.; Li, Y. Geometrical effects in the impact response of the aluminium honeycomb sandwich structures. *J. Reinf. Plast. Compos.* **2014**, *33*, 1148–1157. [[CrossRef](#)]
33. Audibert, C.; Andréani, A.-S.; Lainé, É.; Grandidier, J.-C. Discrete modelling of low-velocity impact on Nomex[®] honeycomb sandwich structures with CFRP skins. *Compos. Struct.* **2019**, *207*, 108–118. [[CrossRef](#)]
34. *Divinycell Technical Manual*; DIAB Group AB: Helsingborg, Sweden, 2010.